CHEMICAL ENGINEERING TRANSACTIONS
VOL. 100, 2023
A publication of AIDIC
The Italian Association of Chemical Engineering
Online at www.cetjournal.it
Guest Editors: Sauro Pierucci, Flavio Manenti

ISBN 979-12-81206-03-8; **ISSN** 2283-9216
DOI: 10.3303/CET23100040

A Thermodynamic/Kinetic Study of Ammonia-based Flue Gas Desulfurization Processes

Domenico Flagiello[a], Francesco Di Natale[a], Amedeo Lancia[a], Ilio Sebastiani[b], Fabrizio Nava[b], Antonino Milicia[b], Alessandro Erto[a]

[a]Department of Chemical, Materials and Production Engineering, University of Naples Federico II – P.le Tecchio 80, 80125 Naples, Italy.
[b]Desmet Ballestra SpA – Via Piero Portaluppi 17 - 20138 Milan, Italy.
domenico.flagiello@unina.it

In this work, we propose a study of the SO_2 mass-transfer rate in an absorption process based on the use of an aqueous solution of ammonia (NH_3), which reacts with SO_2 to give ammonium sulfite according to follow overall reaction $SO_2 + 2NH_3 + H_2O \rightarrow (NH_4)_2SO_3$. An experimental and modelling study is carried out to define the thermodynamic and kinetic aspects of the ammonia-based Flue Gas Desulfurization (FGD) process. A dataset of SO_2 solubility in aqueous ammonia solutions was estimated by simulations in ASPEN PLUS using an equilibrium model based on data provided in the relevant literature. The Enhancement factors (E_L) for the SO_2 ammonia-based absorption are determined under the explored experimental conditions: different gas and liquid flow rates, and feed molar $NH_{3(aq)}/SO_{2(g)}$ ratios, varying both concentrations of ammonia in the liquid and sulfur dioxide in the gas streams.

1. Introduction

The growing energy demand and the need for more sustainable processes make Flue Gas Desulfurization (FGD) processes still a hot topic for Chemical and Environmental Engineering. Nowadays, most of the power generation, industrial activities and marine transportation sector still use fossil fuels for power generation. Even if SO_x emissions can be limited by using low-sulfur fossil-fuels, for several applications after-treatment processes are the only suitable options to comply with the increasingly stringent regulations. These technologies include dry and semi-scrubbers (Ma et al., 2000; Koech et al., 2021) or wet scrubbing columns (Flagiello et al., 2020a; Flagiello et al., 2021a) the latter option being the most effective and well-established.
Sulfur dioxide is very soluble in water, but it can be more efficiently removed from flue-gas using reactive-absorption processes in wet scrubbers. Meanwhile, European Community has set a drastic cut in global SO_x emissions of about 70% to achieve in 2030 (2016/2284/UE) and similar measures have been planned in other countries worldwide (Wynn and Coghe, 2017; Zhang, 2016). Despite the maturity of wet-FGD technologies and the progress achieved to date, an extensive study of the key parameters of traditional or non-traditional FGD processes must be carried out to increase the efficiency and simultaneously optimize the consumption of chemicals, reduce the footprint of plants and water flow required, and consequently reduce the volume of waste effluent.
To date, several traditional chemicals have been adopted (Adewuyi and Sakyi, 2013; Colle et al., 2004; Flagiello et al., 2021b; Flagiello et al., 2022a; Flagiello et al., 2023a; Gutiérrez Ortiz et al., 2006) to improve SO_x removal from flue-gas, including ammonia-based scrubbing, which is widely adopted for FGD in coal-fired power plants operating with high-sulfur content (Gao et al., 2010; Jia et al., 2010; Tang et al., 2017). Further interest in this process is given by the formation of $(NH_4)_2SO_3$ that, when further oxidized in the aqueous-phase and purified into other chemical units, leads to ammonium sulfate $(NH_4)_2SO_4$, which is an important precursor in nitrogen-based fertilizer manufacturing processes (Liu et al., 2011). However, some fundamental aspects about the intrinsic kinetic of the process including kinetic data on the gas-liquid reactions are limited and deserve a dedicated study for process design and optimization on large-scale plants.

Paper Received: 10 December 2022; Revised: 16 March 2023; Accepted: 27 May 2023
Please cite this article as: Flagiello D., Di Natale F., Lancia A., Sebastiani I., Nava F., Milicia A., Erto A., 2023, A Thermodynamic/kinetic Study of Ammonia-based Flue Gas Desulfurization Processes, Chemical Engineering Transactions, 100, 235-240 DOI:10.3303/CET23100040

In the present work, we investigated the wet desulfurization of a model flue-gas at T = 20 °C using aqueous solutions containing ammonia, which promotes a fast reactive-absorption (Gao et al., 2010; Jia et al., 2010), as reported in Eq. (1):

$$SO_{2(aq)} + 2NH_{3(aq)} + H_2O_{(l)} \rightarrow 2NH_4^+ + SO_3^{2-} \quad (1)$$

representing the overall reaction for the SO_2/NH_3 absorption-system. The experiments aimed to evaluate the mass-transfer kinetics determining the Enhancement Factors (E_L) of the SO_2/NH_3 absorption-system at 20 °C. In chemical absorption processes, a gas-liquid reaction is fast when the Hatta number (Ha) is greater than 3 and the Enhancement factor can be written as:

$$E_L = \frac{Ha}{tgh(Ha)} \approx Ha \quad (2)$$

with E_L about equal to Ha number (Zarzycki and Chacuk, 1993).
The main process parameters investigated during the experimental campaign include gas and liquid flow rates, concentrations of sulfur dioxide in the gas and ammonia in the liquid streams, while the temperature was constant at 20 °C. The experiments were performed in a lab-scale falling-film absorber used to investigate SO_2 mass-transfer rates, as it allows highly controlled mass-transfer conditions for a thorough assessment of the fundamental kinetic aspects of an absorption process with fast gas-liquid reaction. To this aim, the absorber unit allows a precise knowledge of the gas-liquid contact surface (a_e [m^2/m^3]) to accurately assess the mass-transfer rates (Flagiello et al., 2023b). The physical contribution to the SO_2 mass transfer rates are known from our previous work, which allowed determining gas-side ($k_{G,SO2}$ [m/s]) and liquid-side ($k_{L,SO2}$ [m/s]) volumetric coefficients (Flagiello et al., 2023b).Also, a thermodynamic study of the SO_2 absorption process is preparatory to the calculation of Enhancement factors. For this purpose, an equilibrium model was developed in ASPEN PLUS, which is based on gas-liquid phase equilibria and liquid-phase chemical equilibrium equations, both retrieved from the relevant literature.

2. Materials and Methods

High pressure cylinders of pure N_2 (5.0 technical grade) and SO_2 at 3040 ppm_v in N_2 (Rivoira Gas, Italy), distilled water and ammonia aqueous solution at 30% w/w (Sigma Aldrich, Italy) were used in the experiments.

2.1 Experimental section

The experimental unit is a continuous liquid-film contactor and consists of a Pyrex glass column (effective gas-liquid contact height, Z = 0.155 m) with 0.018 m internal diameter, and 2 mm thickness. The column also has a Pyrex glass chamber at the top to overflow the liquid from the top to the bottom chamber, in which the liquid is collected. The specific surface area wetted by the liquid-film (a_e) during the experiments is 222 m^2/m^3 calculated by geometric internal surface of the cylinder, considering the liquid-film thickness negligible as compared with the column diameter (Flagiello et al., 2023b).
The model flue-gas at 20 °C is prepared by mixing a pure nitrogen stream with a sulfur dioxide stream available at 3040 ppm_v and using two digital flow meters (0 - 20 NL/min; detection limit of 0.1 NL/min) to regulate flow rates for both gas lines, in order to obtain the desired inlet concentration of SO_2 ($C_{SO2(g),in}$ [ppm_v]).
The absorbing liquid at 20 °C is prepared with the desired concentration of ammonia ($C_{NH3(aq),in}$ [w/w]) and stored in a vessel with a maximum capacity of 15 liters. An immersion pump with a maximum power of 30 W placed inside the tank feeds the liquid to the column that falls on the walls from the top to the bottom. Liquid flow rate ($L_{v,in}$ [L/h]) is controlled by a digital flow meter (0 - 4 L/min; detection limit of 0.01 L/min) and the gas flow rate ($G_{v,in}$ [L/h]) is fed in countercurrent to the liquid. The liquid flowing out the column is discharged into another tank with a maximum capacity of 20 liters.
The concentration of SO_2 in the gas stream at the column outlet ($C_{SO2(g),out}$ [ppm_v]) is monitored over time using a Pollutek Gas Analysis system with dual range 0 - 600 and 0 - 3000 ppm_v with accuracy 0.1 ppm_v and providing 0.1% deviation from the full scale. The experimental apparatus is also equipped with a gas heat exchanger with electrical resistance, a thermoregulating system of the liquid stream measuring and all instruments to record gas temperature, relative humidity and pressure during the experiments, at different sampling points. Further details of the experimental plant and auxiliary equipment, process flow diagram and experimental test procedures can be found in Flagiello et al. (2023b).
The ammonia concentrations used in the experiments were selected based on the investigated gas and liquid flow rates, including SO_2 inlet concentrations to explore a broad range of the feed molar $NH_{3(aq)}/SO_{2(g)}$ ratio (r_{op}), i.e. with NH_3 strongly in defect or in excess respect to SO_2, up to values close to the stoichiometric one (equal

to 2, see Eq. (1)). The main process parameters in the experiments are summarized in Table 1, including the gas-side ($k_{G,SO2}$ [m/s]) and liquid-side ($k_{L,SO2}$ [m/s]) volumetric coefficients calculated by Flagiello et al. (2023b) using the same operating conditions and experimental set-up of the present work.

Table 1: Main process parameters in the absorption experiments with falling-film absorber unit.

T [°C]	P [atm]	$G_{v,in}$ [L/h]	$L_{v,in}$ [L/h]	L/G [L/m^3]	$k_{G,SO2}$ [m/s]	$k_{L,SO2}$ [m/s]	$C_{SO2(g),in}$ [ppm$_v$]	$C_{NH3(aq),in}$ [% w/w]	r_{op} [mol/mol]
20	1.13	503	18	36	$1.79 \cdot 10^{-2}$	$2.06 \cdot 10^{-4}$	from 395 to 2960	$4 \cdot 10^{-3}$ and $1.6 \cdot 10^{-2}$	from 0.62 to 46
	1.08	408	22	54	$1.55 \cdot 10^{-2}$	$1.93 \cdot 10^{-4}$			
	1.05	314	24	76	$1.29 \cdot 10^{-2}$	$1.66 \cdot 10^{-4}$			

2.2 Data Analysis

The experimental absorption results were interpreted according to the classic absorber design equation deriving from the two-film theory for mass-transfer in gas-liquid systems, valid for dilute absorption case with constant temperature and pressure, and written in a generalized canonical form as (Zarzycki and Chacuk, 1993):

$$Z = HTU_{OG} \cdot NTU_{OG} = \left\langle \frac{G_m}{S} \left[\frac{1}{\rho_G k_{G,SO_2} a_e} + \frac{F_{eq,i}}{\rho_L E_L k_{L,SO_2} a_e} \right] \right\rangle_{LM} \cdot \int_{y_{SO_2,out}}^{y_{SO_2,in}} \frac{dy}{(y_{SO_2} - y_{SO_{2(eq)}})} \quad (3)$$

where HTU_{OG} is the Height Transfer Unit representing the overall resistance to mass transfer referred to the gas-phase and is calculated as the logarithmic mean value between the top and bottom of the column, while NTU_{OG} is the Number Transfer Units, written as a function of the gas mole fraction of SO_2 (y_{SO2} [mol/mol]) along the column.

In Eq. (3), Z [m] is the column height, S [m^2] is the column cross section, G_m [kmol/s] is the molar flow rate of the gas, ρ_G [kmol/m^3] is the molar density of the gas, ρ_L [kmol/m^3] is the molar density of the liquid, $y_{SO2,in}$ [mol/mol] is the inlet mole fraction of SO_2 at the bottom of column, $y_{SO2,out}$ [mol/mol] is the outlet mole fraction of SO_2 at the top of column, $y_{SO2(eq)}$ [mol/mol] is the mole fraction of SO_2 in the gas-phase in equilibrium with total sulfur in the liquid-phase ($x_{S(eq)}$), which represents the gas solubility in a given aqueous solution. It is worth noting that the value of the Enhancement factor (E_L) is $E_L > 1$ for chemical absorption with chemical reaction in the liquid-phase, while $F_{eq,i}$ represents the derivative of the equilibrium function that coincides with the gas-liquid interfacial conditions and corresponds to the dimensionless Henry's constant given by the ratio between $K_{H,SO2}$/P, where the Henry's constant for SO_2 in water ($K_{H,SO2}$ [atm]) can be found in Flagiello et al. (2018).

The NTU_{OG} can be calculated from the experimental absorption results ($y_{SO2,out} = C_{SO2(g),out} \cdot 10^{-6}$ mol/mol) and if the equilibrium dataset ($x_{S(eq)}$ - $y_{SO2(eq)}$) for SO_2 absorption in NH_3 solutions is available. This dataset was obtained by simulations using a computational code developed in ASPEN PLUS based on our previous works (Flagiello et al., 2018; Flagiello et al., 2020b) and suitably adapted to the case study of the present work.

Given the $k_{G,SO2}a_e$ and $k_{L,SO2}a_e$ coefficients, evaluated in the same operating conditions and experimental set-up from our previous work, the chemical contribution due to the reaction indicated in Eq. (1) is concentrated in the Enhancement factor (E_L), which can be calculated for each experiment from Eq. (3). It is worth underlining that, since the experimental unit does not allow gas or liquid sampling at intermediate column heights, it is assumed that the E_L calculated from Eq. (3) represents an average value of the experiment. In general, E_L can vary along the column but it is possible to assume a constant value of HTU_{OG} as the average between the column top/bottom in case of fast chemical reaction, because in most cases the liquid-side resistance can be considered as negligible (Flagiello et al., 2023b).

2.3 Equilibrium model for SO_2 absorption in NH_3 solutions implemented in ASPEN PLUS simulator

The computational code developed is a predictive equilibrium model for SO_2 absorption in NH_3 aqueous solutions, based on a set of thermodynamic equilibrium equations (phase equilibria and chemical equilibria). These equations were implemented in the Flash block of ASPEN PLUS (using Elec-NRTL property method) and the values of the related constants are given in Table 2.

The Flash block is a continuous unit working at constant pressure and temperature (i.e. an ideal equilibrium stage) fed by a gaseous stream (nitrogen and sulfur dioxide at the desired concentration) and a liquid stream (water and ammonia at the investigated concentration) and allows to simultaneously solve the mass, energy and charge balance equations.

At the Flash block output, two streams (gas and a liquid) are obtained at thermodynamic equilibrium. By using the sensitivity analysis tool of the process and varying e.g. the liquid flow rate to the Flash block, equilibrium data can be obtained at the fixed NH_3 concentration.

Table 2: Set of equations for the SO_2 absorption model in NH_3 aqueous solutions, including the values of the constants of the phase ($K_{P°}$ and K_H [atm]) and chemical (K_{eq} [mol/mol]^q) equilibria at 20 °C. The exponent q represents the difference between the sum of the stoichiometric coefficients of the products and reactants in the chemical reaction.

Number Equation	Equilibrium Equation	Constant values @ T = 20 °C	References
(4)	$SO_{2(g)} \rightleftharpoons SO_{2(aq)}$	K_H = exp(3.65)	Flagiello et al. (2018)
(5)	$H_2O_{(l)} \rightleftharpoons H_2O_{(g)}$	$K_{P°}$ = exp(-3.71)	Flagiello et al. (2018)
(6)	$NH_{3(aq)} \rightleftharpoons NH_{3(g)}$	K_H = exp(1.61) $K_{P°}$ = exp(2.12)	Luckas et al. (1994)
(7)	$H_2O_{(l)} \rightleftharpoons H_3O^+ + OH^-$	K_{eq} = exp(-40.69)	Flagiello et al. (2018)
(8)	$SO_{2(aq)} + 2H_2O_{(l)} \rightleftharpoons HSO_3^- + H_3O^+$	K_{eq} = exp(-8.11)	Flagiello et al. (2018)
(9)	$HSO_3^- + H_2O_{(l)} \rightleftharpoons SO_3^{2-} + H_3O^+$	K_{eq} = exp(-20.74)	Flagiello et al. (2018)
(10)	$NH_{3(aq)} + H_2O_{(l)} \rightleftharpoons NH_4^+ + OH^-$	K_{eq} = exp(-14.99)	Luckas et al. (1994)

3. Results and Discussion

Figure 1 shows SO_2 outlet concentrations from the falling-film absorber ($C_{SO2(g),out}$) *vs* SO_2 inlet concentrations ($C_{SO2(g),in}$). The results include the influence of liquid-to-gas ratio (L/G) and the ammonia feed concentration: $C_{NH3(aq),in}$ = 4·10^{-3} % w/w in Figure 2a and $C_{NH3(aq),in}$ = 1.6·10^{-2} % w/w in Figure 2b.

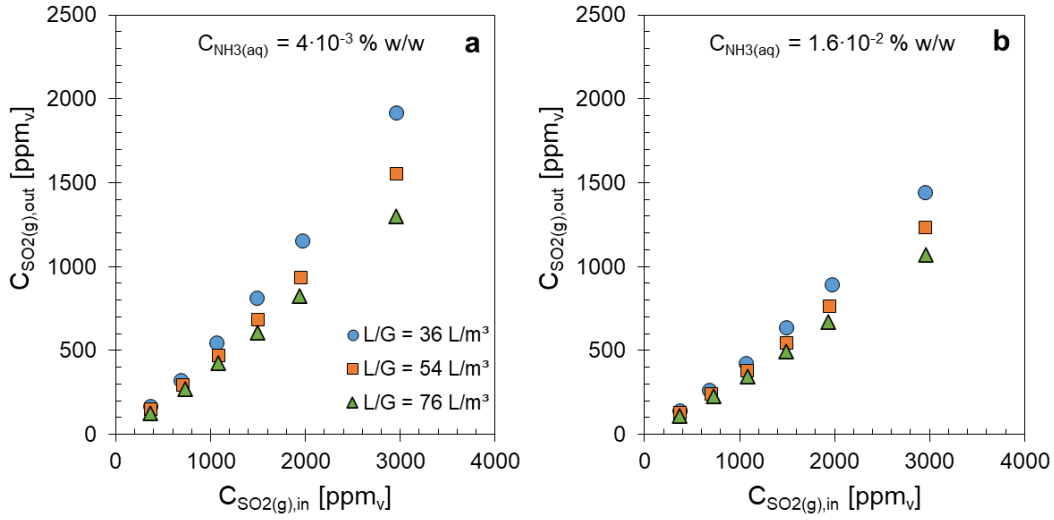

Figure 1: Experimental values of SO_2 outlet concentration as a function of the inlet concentration of SO_2 and liquid-to-gas ratio, parametric with ammonia concentration $C_{NH3(aq)}$ = 4·10^{-3} % w/w (Figure 1a) and $C_{NH3(aq)}$ = 1.6·10^{-2} % w/w (Figure 1b).

From Figure 1, we can see that the outlet concentration of SO_2 from the absorber ($C_{SO2(g),out}$) decreases with decreasing SO_2 feed concentration ($C_{SO2(g),in}$) and a marked effect of L/G ratio is observed only for high $C_{SO2(g),out}$ values, while almost no differences were observed when it was very low. As expected, higher ammonia concentration $C_{NH3(aq),in}$ = 1.6·10^{-2} % w/w (Figure 1b) allowed best desulfurization performances. However, this effect seems to be more pronounced for high $C_{SO2(g),in}$ values, while a smaller difference in performances were observed for lower $C_{SO2(g),in}$ values. This was probably due to the feed molar ratio r_{op} which assumes an higher value than stoichiometric dosage according to reaction in Eq. (1) when $C_{SO2(g),in}$ decreases, thus making the gas-liquid reaction more effective by flattening the desulfurization performance of the film absorber: in these case, we can assume that the absorption is controlled only by the gas-side resistance.

Figure 2 shows the Enhancement factors (E_L), calculated from the experiments using Eq. (3), as a function of SO_2 inlet concentrations ($C_{SO2(g),in}$). The results include the influence of liquid-to-gas ratio (L/G) and the ammonia feed concentration: $C_{NH3(aq),in}$ = 4·10^{-3} % w/w (Figure 2a) and $C_{NH3(aq),in}$ = 1.6·10^{-2} % w/w in (Figure 2b).

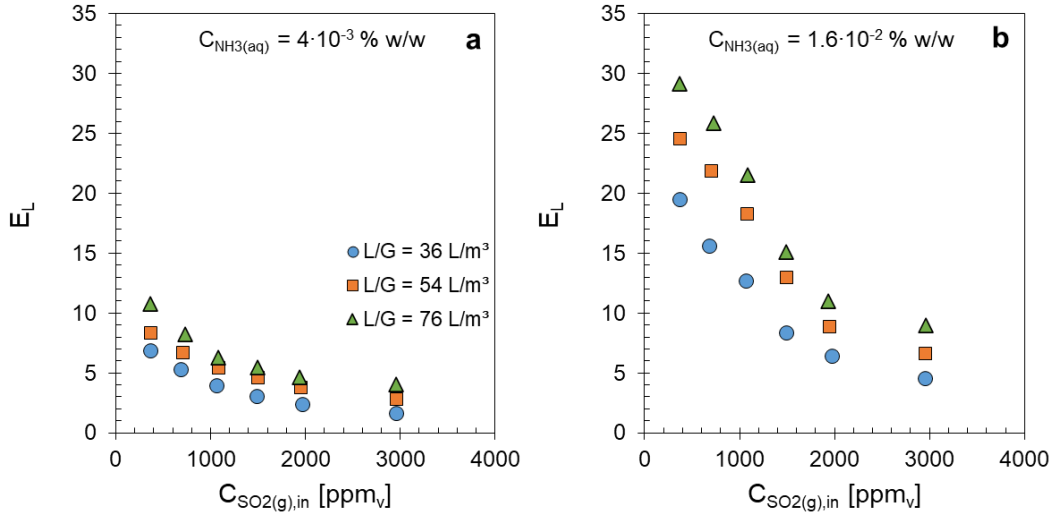

Figure 2: Experimental values of Enhancement Factors as a function of gas inlet concentration of SO_2 and liquid-to-gas ratio, parametric with ammonia concentration $C_{NH3(aq)}$ = 4·10^{-3} % w/w (Figure 2a) and $C_{NH3(aq)}$ = 1.6·10^{-2} % w/w (Figure 2b).

The results show that most Enhancement factors are greater 3, confirming that the gas-liquid reaction follows a fast regime (Eq. (2)) as observed by Gao et al. (2010) and Jia et al. (2010). Only for few experiments a E_L value < 3 was retrieved: this was probably ascribable to feed molar ratio (r_{op}), which in those cases, assumed values more than 50% lower than the stoichiometric value of the overall reaction (Eq. (1)), and consequently a fast reactive-mechanism was not achieved.

From Figure 2, at fixed investigated ammonia concentration, it is observed that the Enhancement factors increased as SO_2 concentration decreased ($C_{SO2(g),in}$) , likely because the feed molar ratio (r_{op}) increased and, consequently, the ammonia available for reactive gas-liquid mechanism increased. The E_L also increases as the investigated L/G ratio increases, which is typical of purely physical absorption but is also a direct consequence of the simultaneous increase in r_{op}. As expected, E_L values were greater for higher ammonia concentration ($C_{NH3(aq),in}$ = 1.6·10^{-2} % w/w), as can be observed in Figure 2b. In particular, a difference of about 75% between the two investigated ammonia concentrations results in 65% difference on average in E_L values, being data reported in Figure 2b significantly greater than those reported in Figure 2a. The difference in ammonia concentration also influenced E_L trends, which grew much faster when the reactive dosage was higher (Figures 2b).

4. Conclusions

This work reports an experimental and modelling study of the kinetics of SO_2 absorption in aqueous solutions containing ammonia in a wide range of feed molar $NH_{3(aq)}/SO_{2(g)}$ ratios to investigate reaction kinetics, i.e. with ammonia concentrations ranging from stoichiometric defect to excess dosages, with respect to sulfur dioxide. The experimental activity allowed determining the Enhancement factor for SO_2/NH_3 absorption system, which represents the contribution of the chemical reaction to SO_2 absorption and oxidation to ammonium sulfite. To calculate E_L, it was also necessary to develop a thermodynamic model in ASPEN PLUS to predict SO_2 solubility data in ammonia solutions.

We found that Enhancement factors increased when ammonia feed concentration increased and SO_2 feed concentration decreased. The E_L values confirmed that the gas-liquid reaction provides a fast reactive regime, while the feed molar $NH_{3(aq)}/SO_{2(g)}$ ratio (r_{op}) that included the effect of L/G, $C_{SO2(g),in}$ and $C_{NH3(aq),in}$ could be defined as a key parameter of the process. As expected, the Enhancement factors increased when the dosage ratio r_{op} increased: for low r_{op} values, the desulfurization performances strictly depended on the L/G ratio likely because E_L assumed low values and, consequently, the process was more influenced by physical absorption mechanisms. On the contrary, for higher r_{op}, the chemical absorption mechanisms dominated, so that the L/G ratio did not significantly influence the process.

The experimental activity proposed in the present work can be proficiently applied in the design of ammonia-based FGD scrubbers on larger scale to correctly estimate water and chemicals demand, aimed at a minimization of plant footprint and waste effluents production. However, this is a first step and a more detailed kinetic study on typical wet-scrubber operating temperatures must be performed. In addition, the development of a predictive model for E_L by isolating the contribution of the chemical reaction (reaction kinetics) from the physical contribution to mass-transfer ($k_G a_e$ and $k_L a_e$) is needed. In general, this approach based on extensive kinetic studies could make wet-desulfurization processes less energy-intensive and costly and consequently more sustainable.

References

Adewuyi Y.G. and Sakyi N.Y., 2013, Simultaneous absorption and oxidation of nitric oxide and sulfur dioxide by aqueous solutions of sodium persulfate activated by temperature, Ind. Eng. Chem. Res., 52, 11702–11711.

Colle S., Vanderschuren J., Thomas D., 2004, Pilot-scale validation of the kinetics of SO_2 absorption into sulphuric acid solutions containing hydrogen peroxide, Chem. Eng. Process.: Process Intensif., 43, 1397–1402.

Flagiello D., Erto A., Lancia A., Di Natale, F., 2018, Experimental and modelling analysis of seawater scrubbers for sulphur dioxide removal from flue-gas, Fuel, 214, 254–263.

Flagiello D., Erto A., Lancia A., Di Natale F., 2020a, Dataset of wet desulphurization scrubbing in a column packed with Mellapak 250.X, Data in Brief, 33, 106383.

Flagiello D., Di Natale F., Erto A., Lancia A., 2020b, Wet oxidation scrubbing (WOS) for flue-gas desulphurization using sodium chlorite seawater solutions, Fuel, 277, 118055.

Flagiello D., Di Natale F., Lancia A., Salo K., 2021a, Effect of Seawater Alkalinity on the Performances of a Marine Diesel Engine Desulphurization Scrubber, Chemical Engineering Transaction, 86, 505–510.

Flagiello D., Esposito M., Di Natale F., Salo K., 2021b, A Novel Approach to Reduce the Environmental Footprint of Maritime Shipping, J. Mar. Sci. Appl., 20, 229–247.

Flagiello D., Erto A., Lancia A., Di Natale F., 2022a, Advanced Flue-Gas cleaning by wet oxidative scrubbing (WOS) using $NaClO_2$ aqueous solutions, J. Chem. Eng., 447, 137585.

Flagiello D., Lancia A., Erto A., Di Natale F., 2023a, Advanced exhaust-gas scrubbing for simultaneous de-SO_x/NO_x using a wet oxidative process with integrated washwater treatment, Chem. Eng. Res. Des., 194, 731–741.

Flagiello D., Di Natale F., Lancia A., Sebastiani I., Nava F., Milicia A., Erto A., 2023b, Experimental and modelling approach to the design of chemical absorption columns with fast gas-liquid reaction: A case-study on flue-gas desulfurization with H_2O_2 oxidative solutions, Chem. Eng. Res. Des., 194, 425–438.

Gao X., Ding H., Du Z., Wu Z., Fang M., Luo Z., Cen, K., 2010, Gas–liquid absorption reaction between $(NH_4)_2SO_3$ solution and SO_2 for ammonia-based wet flue gas desulfurization, Appl. Energy, 87, 2647–2651.

Gutiérrez Ortiz F.J., Vidal F., Ollero P., Salvador L., Cortés V., Gimenez, A., 2006, Pilot-plant technical assessment of wet flue gas desulfurization using limestone, Ind. Eng. Chem. Res., 45, 1466–1477.

Jia Y., Zhong Q., Fan X., Wang X., 2010, Kinetics of oxidation of total sulfite in the ammonia-based wet flue gas desulfurization process, J. Chem. Eng., 164, 132–138.

Koech L., Rutto H., Lerotholi L., Everson R.C., Neomagus H., Branken D., Moganelwa A., 2021, Spray drying absorption for desulphurization: a review of recent developments, Clean Technologies and Environmental Policy, 23, 1665–1686.

Liu X., Zhong Q., Wang J., Ji X., Jia Y., Xu Y., Li L., 2011, Study on ammonium sulfate crystallization in the ammonium desulphurization process in a coal-based power plant in the petrochemical industry, Energy Sources, Part A: Recovery, Utilization, and Environmental Effects, 33, 2027–2035.

Luckas M., Lucas K., Roth, H., 1994, Computation of phase and chemical equilibria in flue-gas/water systems, AIChE journal, 40, 1892–1900.

Ma X., Kaneko T., Tashimo T., Yoshida T., Kato K., 2000, Use of limestone for SO_2 removal from flue gas in the semidry FGD process with a powder-particle spouted bed, Chem. Eng. Sci., 55, 4643–4652.

Tang Y., Gao Y., Liu D., Zhang F., Qu S., Hao Z., Zhang X., Liu Z.T., 2017, Modeling and simulation of an improved ammonia-based desulfurization process for Claus tail gas treatment, RSC advances, 7, 23591–23599.

Wynn G., and Coghe, P., 2017, Europe's Coal-Fired Power Plant: Rough Times Ahead, Institute for Energy Economics and Financial Analysis, Report published on May.

Zarzycki R. and Chacuk A., 1993, Absorption: fundamentals & applications, Pergamon Press, Oxford, UK.

Zhang X., 2016, Emission standards and control of PM2.5 from coal-fired power plant, IEA Clean Coal Centre, London.